Quantum Monte Carlo study of small aluminum clusters Al_n ($n = 2$–13)

Ladir Cândido* and J. N. Teixeira Rabelo†
Instituto de Física, Universidade Federal de Goiás Campus Samambaia, 74001-970, Goiânia, GO, Brazil

Juarez L. F. Da Silva‡
Instituto de Física de São Carlos, Universidade de São Paulo, Caixa Postal 369, 13560-970, São Carlos, SP, Brazil and
Instituto de Química de São Carlos, Universidade de São Paulo, Caixa Postal 780, 13560-970, São Carlos, SP, Brazil

Guo-Qiang Hai§
Instituto de Física de São Carlos, Universidade de São Paulo, 13560-970, São Carlos, SP, Brazil
(Received 1 February 2012; revised manuscript received 10 April 2012; published 5 June 2012)

Using fixed node diffusion quantum Monte Carlo (FN-DMC) simulations and density functional theory (DFT) within the generalized gradient approximations, we calculate the total energies of the relaxed and unrelaxed neutral, cationic, and anionic aluminum clusters, Al_n ($n = 1$–13). From the obtained total energies, we extract the ionization potential and electron detachment energy and compare with previous theoretical and experimental results. Our results for the electronic properties from both the FN-DMC and DFT calculations are in reasonably good agreement with the available experimental data. A comparison between the FN-DMC and DFT results reveals that their differences are a few tenths of electron volt for both the ionization potential and the electron detachment energy. We also observe two distinct behaviors in the electron correlation contribution to the total energies from smaller to larger clusters, which could be assigned to the structural transition of the clusters from planar to three-dimensional occurring at $n = 4$ to 5.

DOI: 10.1103/PhysRevB.85.245404 PACS number(s): 61.46.Bc, 36.40.−c, 02.70.Ss, 32.10.Hq

I. INTRODUCTION

In the last two decades, aluminum clusters, Al_n, have attracted great interest due to their fascinating physical and chemical properties as well as the possibility of new technological applications.[1–5] For instance, Al_7^+ and Al_{13}^- are considered to be the magic clusters as they contain 20 and 40 valence electrons, respectively, with closed-shell structures. While Al_{13}^0 shows remarkable properties such as the superhalogen behavior with a very high electron affinity exceeding those of halogen atoms.[6,7] A recent experimental study[8] on the reactivity of anionic clusters Al_n^- with water demonstrates that their reactivity varies sharply with cluster size. Certain clusters, such as Al_{16}^-, Al_{17}^-, and Al_{18}^-, with geometric structure of multiple active sites result in production of H_2 from water. It indicates that these anionic Al clusters can be potentially applied in water splitting. Furthermore, the size-dependent fluctuations in the melting temperatures and latent heats of Al clusters have attracted much attention for clusters with less than a few hundred atoms.[9,10] Changing the cluster size by even a single atom can cause a substantial difference in the melting behavior.

Considerable effort has been made in trying to understand the properties of the Al clusters and their size dependence. Experimentally measurable quantities such as ionization potential (IP), electron affinity (EA), and detachment energy (DE) of Al_n clusters play essential roles to reach an atomistic understanding of their stability and reactivity.[6,10,11] In last years, several experimental and theoretical studies have been carried out to obtain the IP, EA, and DE of Al_n clusters as a function of their atomic size (number of atoms). Experimentally, they are usually obtained by using pulsed cluster beam flow reactor[12] and photoelectron spectroscopy techniques.[13–15] Theoretical calculations are mostly based on density functional theory.[6,16–20] These studies have provided valuable information for our understanding on the Al_n clusters. However, due to lack of accuracy both in theoretical and experimental techniques, it is still challenging to obtain their values in chemical accuracy.

Density functional theory (DFT) with approximated local and semilocal exchange-correlation (xc) energy functionals is currently the standard approach for computing materials properties and has been successful in studies for a wide range of materials. However, there exists no method to estimate the errors resulting from the approximations in xc energy used in DFT. It is often doubtful on the accuracy of calculated results within DFT at describing a given property of materials.[21]

In order to obtain theoretical results with better precision and clarify previous theoretical calculations, in this work, we employ fixed node diffusion quantum Monte Carlo (FN-DMC) method to study the electronic structure of the Al_n clusters ($n = 1$–13) in comparison with the DFT calculations. In quantum Monte Carlo (QMC) method, one solves the full many-body Schrödinger equation stochastically within controlled approximations. In principle, the QMC calculation eliminates those uncertainties presented in the DFT and, consequently, can yield more accurate results providing a valuable benchmark.

This paper is organized as follows. In Sec. II, we outline the theoretical approaches for determination of the atomic structures and calculation of the total energy of the Al clusters. In Sec. III, we present the general results of the atomic structures using the coordination number concept. The total energies of the Al clusters in different states are obtained and, consequently, the ionization potentials and electron detachment energies. We also discuss the electron correlation contribution in these systems. We draw our conclusions in Sec. IV.

II. THEORETICAL APPROACHES AND COMPUTATIONAL DETAILS

We combine DFT and QMC calculations to address the atomic structures and electronic properties of the aluminum clusters. The atomic structure will be described by plain DFT within the semilocal xc functional. The total energies of the clusters will be calculated within the QMC method. Such a combination is necessary due to the high computational cost of the QMC calculations. From the obtained energies of the Al_n clusters in different states, we extract the ionization potential (IP) and electron detachment energy (DE).

A. Atomic structure of Al_n clusters

The knowledge of the atomic structures of the Al_n clusters plays a crucial role in the agreement between theoretical calculations and experimental data. The atomic structures of the neutral, cationic, and anionic Al_n clusters are calculated from first-principles molecular dynamics (MD) simulations based on DFT[22,23] within the generalized gradient approximation[24] (GGA) proposed by Perdew, Burke, and Ernzerhof (PBE),[25] and the projected augmented wave (PAW) method[26] as implemented in the Vienna *ab initio* simulation package (VASP).[27,28] A plane-wave cutoff energy of 240 eV was used for all VASP calculations within a cubic box of 14 Å and the Γ point for the Brillouin zone integration.

For the MD simulations, we use a time step of 1.0 fs, and the simulations are run for 10 picoseconds going from high temperature (1000 K) to approximately zero temperature. Several snapshots are selected along the simulation and optimize by local optimizers such as the conjugated gradient as implemented in VASP. This procedure has been used in several studies with great success.[29,30] An anionic (cationic) Al_n cluster is obtained by adding (removing) one electron to (from) the neutral one and a complete geometric relaxation is performed.

B. DFT-PBE and FN-DMC

The total energies of the Al_n clusters in different states, which are required to obtain the IP and DE, are calculated within the DFT-PBE and FN-DMC. In order to discuss the effects of electron correlation, we also calculate the total energies of the clusters within the Hartree-Fock (HF) approximation. In the calculations of the HF and DFT-PBE total energies, we use the GAUSSIAN03 package,[31] with the GEN basis set, i.e., a 6-311G$++(2d,2p)$ with valence triple ζ + double polarization + diffuse on all atoms (VTZ2PD) from the site EMSL basis set exchange.[32]

The QMC calculations are performed using the widely used CASINO code.[33] In the calculations, the core electrons are modeled by an effective core potential, namely, the Dirac-Fock average relativistic effective potential (AREP)[34] as provided in CASINO. The variational Monte Carlo (VMC) trail wave functions are of the Slater-Jastrow type,

$$\psi_{\mathrm{T}}(R) = D_{\uparrow}(\phi_i)D_{\downarrow}(\phi_i)e^{U}, \tag{1}$$

where R is the electronic configuration, $D_{\uparrow\downarrow}$ are determinants of up- and down-spin orbitals, ϕ's are the single-particle orbitals with five s, five p, one sp, and three d functions, which are extracted from a DFT calculation using the GAUSSIAN03 code.[31]

The Jastrow factor U in Eq. (1) is a sum of homogeneous, isotropic electron-electron terms $u(r_{ij},\alpha)$, isotropic electron-core terms $\chi(r_{iI},\beta)$ centered on the core and isotropic electron-electron-core terms $f(r_{iI},r_{jI},r_{ij};\gamma)$, where $r_{ij} = r_i - r_j$ and $r_{iI} = r_i - r_I$, r_i is the position of the electron i and r_I is the position of the core I. The α, β, and γ represent about 80 variational parameters, which are optimized for each Al_n cluster structure using the method of variance minimization,

$$\sigma^2 = \sum_{i=1}^{M}[E_{\mathrm{L}}(R_i) - E_{\mathrm{VMC}}]/M, \tag{2}$$

where $E_{\mathrm{L}} = H\psi_{\mathrm{T}}(R_i)/\psi_{\mathrm{T}}(R_M)$ with M being the number of samples and H is the Hamiltonian of the system within the Born-Oppenheimer approximation. E_{VMC} is the variational energy evaluated by multidimensional Monte Carlo integration using samples of the electron positions distributed according to $|\psi_{\mathrm{T}}(R)|^2$.

In the diffusion Monte Carlo (DMC) calculation, the optimized trial VMC wave function is used as a guide wave function for importance sampling.[35] In this method, one uses the operator e^{-tH} with $t = i\tau$ to propagate the trial wave function, ψ_{T}, in imaginary time at the long time limit, $t \to \infty$, to project out the system ground state or equivalently, ψ_0. We have used the fixed node approximation that assumes that the nodes of the DMC solution (the nodes of ψ_0) are equal to the nodes of the trial wave function. For the FN-DMC, we have used a time step of 0.001 a.u., which yields calculations with a high acceptance ratio, e.g., larger than 99.99%, and an ensemble of 10 000 walkers is used. For the averages in the FN-DMC calculations, we consider about 50 000 QMC moves.

III. RESULTS AND DISCUSSION

A. Atomic structure

Our first goal is the identification of the putative lowest energy atomic structures for the Al_n ($n = 2$–13) clusters in the neutral, cationic, and anionic states. We employ the following approaches: (i) first-principles MD simulations based on the DFT-PBE framework as implemented in VASP[27,28,36] are performed for the neutral clusters. The selected snapshots (atomic configurations) are optimized using DFT-PBE as implemented in VASP and are reoptimized using GAUSSIAN03 for basis set consistency. (ii) Atomic structures from literature[16] are optimized using DFT-PBE as implemented in GAUSSIAN03. (iii) The relaxed cationic (anionic) clusters are obtained by removing (adding) one electron from (to) the corresponding neutral Al_n clusters and, then, a complete relaxation is performed for each configuration. For particular clusters, the MD simulations are also performed for cationic and anionic clusters for cross check of the obtained geometry. Following these procedures, a large number of atomic configurations are calculated. The obtained lowest energy Al_n ($n = 2$–13) cluster configurations are shown in Fig. 1.

The atomic structures of the Al_n clusters are characterized by using the effective coordination concept.[37,38] In the effective coordination concept, a different weight is calculated for each

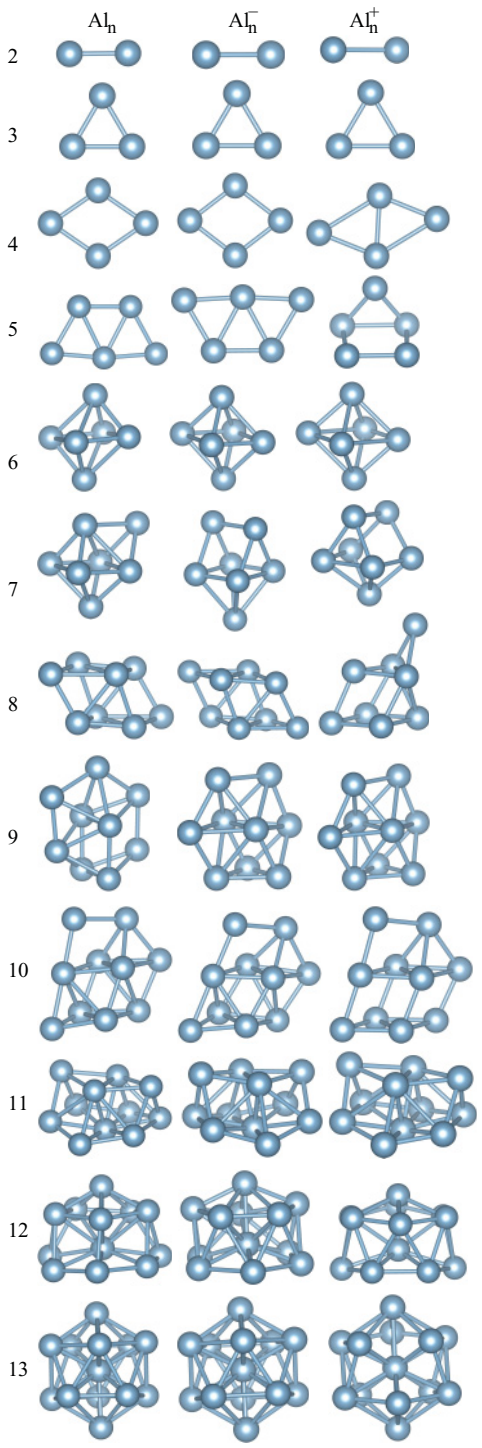

FIG. 1. (Color online) The lowest energy structures of the neutral (Al_n^0), anionic (Al_n^-), and cationic (Al_n^+) clusters obtained within the DFT-PBE as implemented in VASP and GAUSSIAN03.

bond length d_{ij} by using a weight function, i.e., $w_{ij} \neq 1.0$ for all ij.[37,38] This approach is based on the fact that an atom binds stronger with closer atoms, and hence, small changes in the coordination environments can be taken into account. All w_{ij} are calculated with respect to the atom weighted bond length $d_{\rm av}^i$, which must be calculated for each atom i. Thus bond length smaller (larger) than the local weighted bond length $d_{\rm av}^i$ contributes with a w_{ij} larger (smaller) than the unit. The effective coordination number ECN_i is obtained by the sum of all weights w_{ij} and, consequently, it is not necessarily an integer value. This concept can be applied for symmetric or distorted structures consistently. We would like to mention that this approach has been used in the study of transparent conducting oxides[29,39] and transition-metal clusters[30,40] with great success. The results for $d_{\rm av}$ and ECN are summarized in Table I.

TABLE I. Weighted average bond lengths ($d_{\rm av}$) and average effective coordination number (ECN) for the Al_n^0, Al_n^-, and Al_n^+ clusters. The respective atomic structures are shown in Fig. 1.

	$d_{\rm av}$ (Å)			ECN		
n	Al_n^0	Al_n^-	Al_n^+	Al_n^0	Al_n^-	Al_n^+
2	2.51	2.61	2.82	1.00	1.00	1.00
3	2.55	2.55	2.72	2.00	2.00	2.00
4	2.62	2.60	2.79	2.36	2.17	2.07
5	2.61	2.63	2.65	2.64	2.76	2.30
6	2.70	2.72	2.72	3.38	3.91	3.20
7	2.69	2.68	2.64	4.04	3.48	3.42
8	2.68	2.69	2.68	3.81	3.84	3.71
9	2.72	2.72	2.72	4.56	4.55	4.55
10	2.69	2.71	2.69	4.35	4.65	4.20
11	2.72	2.71	2.72	4.99	4.94	4.95
12	2.68	2.74	2.69	5.06	5.52	5.05
13	2.77	2.78	2.75	6.27	6.40	5.71

We observe that for Al_2, the bond lengths of the anionic and cationic structures are 3.98% and 12.35% larger, respectively, than that of the neutral configuration, while the changes are small for Al_3. The Al_4 and the neutral and anionic Al_5 clusters form planar structures. But the structure of the cationic Al_5 cluster is three dimensional (3D). For $n > 5$, all the Al_n clusters present in 3D structures in consistency with previous studies.[16] For larger Al_n clusters, the average bond lengths differ slightly among the neutral, anionic, and cationic clusters, e.g., $d_{\rm av} =$ 2.77, 2.78, 2.75 Å for Al_{13}^0, Al_{13}^-, and Al_{13}^+, respectively. We also find that the ECN of a cationic cluster is always smaller than that of the corresponding neutral one. But the same does not hold for the anionic clusters. These results indicate that the atomic structures of the clusters are indeed affected by gain or loss of a single electron.

B. Total energy

Based on the above atomic structures, we calculate the total energies of the Al_n clusters within the FN-DMC method and DFT-PBE. We choose the DFT-PBE wave functions instead of the HF as the best orbital for the aluminum cluster in the FN-DMC calculation. There are a few sources of error in the FN-DMC calculation such as the inaccuracy of the pseudopotential, the fixed node error as well as the nonlocal term approximations in the FN-DMC method. It is believed that the largest among them is the fixed node approximation. Thus, in order to ensure the accuracy of our calculations, we have performed several tests for variational Monte Carlo (VMC) and FN-DMC by using different orbitals from the HF and DFT-PBE. The trial wave functions from the DFT orbitals result in lower energies for VMC and FN-DMC instead of HF

TABLE II. Total energies (in a.u.) calculated within the DFT-PBE (GAUSSIAN03) and FN-DMC (CASINO) for the relaxed clusters Al_n^0, Al_n^-, and Al_n^+, and for the unrelaxed clusters: $Al_n^{0,-}$ (neutral cluster with the anionic geometry: Al_n^- − 1 electron) and $Al_n^{+,0}$ (cationic cluster with the neutral geometry: Al_n^0 − 1 electron). The digits in parentheses are estimated standard errors in the last decimal places.

		Relaxed structure			Unrelaxed structure	
Method	n	Al_n^0	Al_n^-	Al_n^+	$Al_n^{0,-}$	$Al_n^{+,0}$
DFT-PBE	1	− 1.93558	− 1.95425	− 1.71371	− 1.93558	− 1.71371
	2	− 3.93089	− 3.98573	− 3.70934	− 3.93003	− 3.68737
	3	− 5.95248	− 6.01546	− 5.71953	− 5.95247	− 5.71508
	4	− 7.97167	− 8.04834	− 7.73688	− 7.97018	− 7.73156
	5	− 10.00239	− 10.07918	− 9.76838	− 10.00033	− 9.76067
	6	− 12.05474	− 12.14643	− 11.81385	− 12.05216	− 11.81385
	7	− 14.11783	− 14.19540	− 13.90489	− 14.10767	− 13.88742
	8	− 16.13937	− 16.21718	− 15.91240	− 16.13327	− 15.90639
	9	− 18.17841	− 18.27406	− 17.95516	− 18.17290	− 17.93922
	10	− 20.21440	− 20.30890	− 19.99189	− 20.20682	− 19.98593
	11	− 22.26452	− 22.36111	− 22.03720	− 22.25884	− 22.03422
	12	− 24.31325	− 24.41121	− 24.09155	− 24.30969	− 24.08482
	13	− 26.39686	− 26.51931	− 26.16027	− 26.38834	− 26.14704
FN-DMC	1	− 1.9366(1)	− 1.9526(3)	− 1.71822(4)	− 1.9366(1)	− 1.71822(4)
	2	− 3.9254(2)	− 3.9843(1)	− 3.70791(9)	− 3.9249(2)	− 3.6845(1)
	3	− 5.9509(2)	− 6.0172(3)	− 5.7107(2)	− 5.9490(4)	− 5.7084(2)
	4	− 7.9631(4)	− 8.0438(6)	− 7.7220(6)	− 7.9529(6)	− 7.7180(6)
	5	− 9.9925(6)	− 10.0730(3)	− 9.7567(3)	− 9.9892(4)	− 9.7513(4)
	6	− 12.0422(6)	− 12.1407(5)	− 11.7983(2)	− 12.0322(7)	− 11.7938(4)
	7	− 14.1030(13)	− 14.1855(13)	− 13.8937(3)	− 14.0934(6)	− 13.8762(9)
	8	− 16.1256(10)	− 16.2008(6)	− 15.8944(6)	− 16.1150(8)	− 15.8926(16)
	9	− 18.1596(5)	− 18.2607(7)	− 17.9334(6)	− 18.1524(29)	− 17.9185(10)
	10	− 20.1997(10)	− 20.2912(11)	− 19.9677(10)	− 20.1855(25)	− 19.9606(13)
	11	− 22.2392(13)	− 22.3408(10)	− 22.0109(7)	− 22.2297(14)	− 22.0073(17)
	12	− 24.2941(11)	− 24.3856(12)	− 24.0633(12)	− 24.2857(7)	− 24.0585(7)
	13	− 26.3613(8)	− 26.4943(9)	− 26.1237(12)	− 26.3477(27)	− 26.1088(23)

ones. Furthermore, we have also performed several tests with basis sets of different sizes for the orbital. This error is expected to be small because the many-body electron wave function is represented by the distribution of an ensemble of electrons and the basis set in the FN-DMC is just used to expand the guide wave function that is required for importance sampling. No significant quantitative influence of the basis set on the total energy is found.

Table II summarizes the obtained total energies for the neutral, anionic, and cationic Al_n ($n = 1, \ldots, 13$) clusters with relaxed and unrelaxed structures. For the unrelaxed clusters, we consider the neutral cluster with the anionic geometry $Al_n^{0,-}$ (i.e., Al_n^- − 1 electron) and the cationic cluster with the neutral geometry $Al_n^{+,0}$ (i.e., Al_n^0 − 1 electron).

C. Electron correlation contribution

In this section, we analyze the contribution of the electron correlation to the total energy of the Al_n cluster. In general, the ground-state energy of Al_n can be defined as

$$E_{\mathrm{TOT}} = E_{\mathrm{HF}} + E_{\mathrm{C}}, \tag{3}$$

where E_{TOT} is the total energy of the cluster, E_{HF} is the Hartree-Fock energy, and E_{C} is the correlation energy. Here, we assume the FN-DMC energy as being the total energy of the cluster. Figure 2 shows the relative contribution of the electron correlation denoted by $\gamma(n) = [E_{\mathrm{DMC}}(n) - E_{\mathrm{HF}}(n)]/E_{\mathrm{DMC}}(n)$ as a function of the cluster size. The correlation energies of the different clusters are of similar dependence on their size. They increase as the cluster size increases. However, the relative contribution of the electron correlation $\gamma(n)$ increases faster for $n \leqslant 4$.

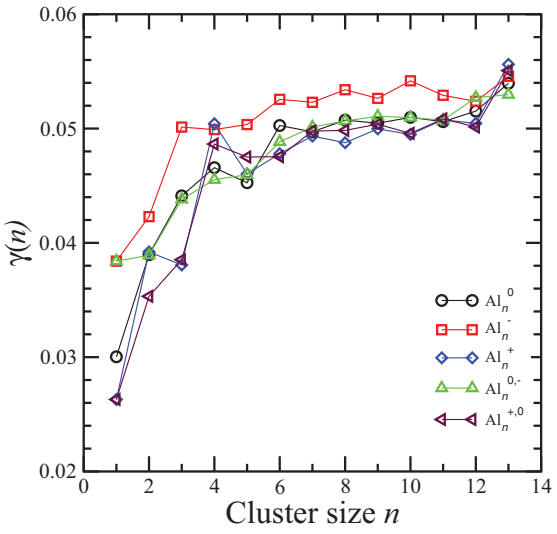

FIG. 2. (Color online) Dependence of the relative electron correlation energy on the cluster size.

For small clusters ($n \leqslant 4$), the electron orbital is small and consequently more localized. In this case, the electron correlation is strong enough leading to a high spin configuration ground state of the cluster. This can be confirmed by the spin multiplicity $m = 2S + 1$ (where S is the total spin) of the ground states of the Al_n clusters. For $n = 1$, $m = 2,3,1$ for neutral, anionic, and cationic clusters, respectively: for $n = 2$, $m = 3,4,2$; for $n = 3$, $m = 2,1,3$; and for $n = 4$, $m = 3,2,4$. For larger clusters ($n > 4$), the system ground state spin arrangement prefer only singlets or doublets so that the total energy is minimized. The electron correlation still increases but slower as the cluster size increases. It can be explained by the fact that the diameter of the electron orbital increases with increasing the system size. The distinct behaviors of the correlation energy for smaller and larger clusters can be assigned to the feature of the atomic transition from planar to 3D structures. We also notice that, among the relaxed structures, i.e., neutral, anionic, and cationic, the largest contribution to the correlation energy is for the anionic system (open red squares), which is reasonable since this system has one electron more.

D. Ionization potential

The IP is given by the difference between the ground-state energies of the neutral and the ionized clusters:

$$\mathrm{IP} = E_n^+ - E_n. \tag{4}$$

If the cationic cluster energy E_n^+ is calculated with the corresponding neutral cluster structure, i.e., without relaxation, the IP is known as vertical IP (VIP). If the structure relaxation due to loss of the electron is taken into account, the IP is the so-called adiabatic IP (AIP).

The obtained VIP and AIP from our calculations are shown in Fig. 3 together with previous theoretical results[16] (for $n = 2-10$) within the DFT-B3LYP and available experimental results.[12] The largest difference (about 0.5 eV) between our results and those from Ref. 16 is found in the VIP at $n = 2$. Because only the lower and upper bounds of the IP were obtained in the experiment,[12] they are indicated by bars in the figure. We also validate the accuracy of our FN-DMC calculations by comparing the obtained energies directly with the experimental data. In general, our results are in good agreement with the experimental data, i.e., the trends are properly described within the error bars. The calculated VIP is a little larger than the AIP. Quantitatively, the AIP obtained from the FN-DMC calculations are in better agreement with the experimental results. But the sharp jump from $n = 6$ to 7 in the theoretical IP (a peak at $n = 6$ and a deep minimum at $n = 7$) was not observed in the experiment. This jump can be understood in terms of the shell structure of the valence electrons. Al_6^0 is a close-shell system, whereas Al_7^0 is a open-shell system with one unpaired electron that can be easily loosed to form Al_7^+. Notice that Al_6 is of the largest AIP (6.64 ± 0.02 eV) but the largest VIP is found for Al_{13} cluster of value 6.87 ± 0.09 eV. The IP obtained from the DFT-PBE calculations is also very close to the experimental data because the differences between the DFT-PBE and the FN-DMC ionized potentials are only a few tenths of electron volt. Such an agreement is mainly due to error cancellation in the total energy differences. We also see that the alternations in the DFT-PBE ionization potentials as a function of the cluster size are very different from those in the FN-DMC. For example, the FN-DMC calculations indicate that both the VIP and AIP of Al_{11} are smaller than those of its neighbors Al_{10} and Al_{12}, but the DFT-PBE shows opposite.

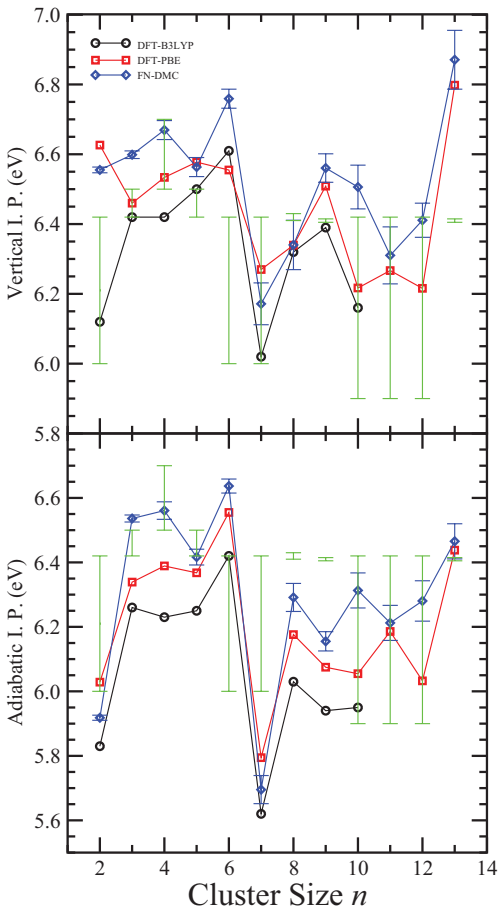

FIG. 3. (Color online) Comparison of the obtained vertical and adiabatic ionization potentials of the Al_n clusters with previously calculated results from Ref. 16 within the DFT-B3LYP and experimental measurements (the vertical green bars) from Ref. 12. The same experimental data are used in the two figures.

E. Detachment energy

The electron detachment energy is the energy difference between the anionic and neutral clusters:

$$\mathrm{DE} = E_n - E_n^-. \tag{5}$$

When both the energies of the anionic and neutral clusters are calculated from the relaxed structures, we obtain the adiabatic detachment energy (ADE). To study the vertical electron detachment energy (VDE), we have also to calculate the total energy of the neutral cluster with the geometry of the Al_n^-. The FN-DMC and DFT-PBE results for the ADE and VDE are compared with experimental measurements[15] in Fig. 4. In comparison with the errors appeared in the IP (see Fig. 3), the experimental data of the DE have a better accuracy with an uncertainty of about 0.1 eV.

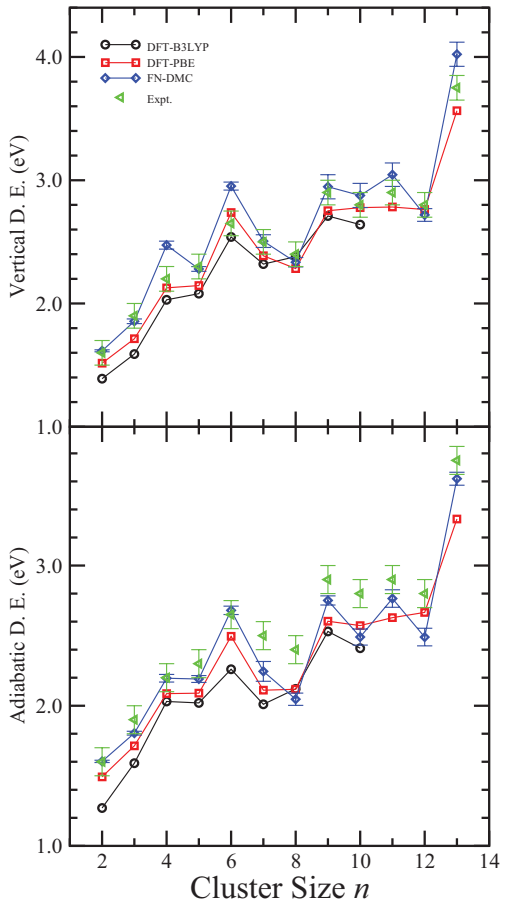

FIG. 4. (Color online) Comparison of the vertical and adiabatic electron detachment energies of the Al_n clusters with previously calculated results within the DFT-B3LYP from Ref. 16 and experimental data from Ref. 15. Note that the same experimental data are used to compare with the theoretical VDE and ADE.

The FN-DMC and DFT results for the VDE and ADE follow the experimental trends.[13–16] The theoretical results from different approaches are close to each other within a few tenths of electron volt. Our calculation results of the VDE and ADE are slightly larger than those obtained in Ref. 16 within the DFT-B3LYP except Al_8. We consider, in general, both the FN-DMC and DFT-PBE results are in good agreement with the experimental data.[15] However the FN-DMC calculations, which are more reliable, show the ADE in better agreement with experiments. Obvious differences between the FN-DMC and DFT-PBE results can be seen in the alternations of the DE for $n > 8$. In addition, the obtained VDE and ADE increases almost linearly for the cluster size from $n = 2$ to 4. For $n > 4$, an alternation is present, especially, in the FN-DMC results. This reflects alternation between singlet and doublet in the ground states of the clusters. The absence of alternation for small clusters arises because the strong electron-electron correlation affects the orbital occupation leading the cluster ground states to prefer higher spin multiplicities, as discussed in Sec. II C. The VDE and ADE of Al_{13} are 3.989 ± 0.098 and 3.619 ± 0.046 eV, respectively, and much larger than the others.

IV. SUMMARY

In this work, we have determined the impact of the electron correlation on the structural and electronic properties of small aluminum clusters using high-accuracy QMC simulations and examined the reliability of the DFT calculations on the ionization potential and electron detachment energy. We obtained the total energy, ionization potential and electron detachment energy of aluminum clusters Al_n ($n = 1$–13) within different theoretical frameworks, namely, the FN-DMC and DFT-PBE. We found that the differences between the DFT-PBE and FN-DMC results are only a few tenths of electron volt. However, such a difference can lead to different alternations in the ionization potential and detachment energy as a function of the cluster size.

The important feature in our theoretical calculations lies in small numerical errors and quite good quantitative agreement with the experimental data. This indicates that the computationally predicted structures are very close to the experimental ones. Also, the analysis of the relative electron correlation contribution to the total energy shows two distinct regimes for smaller and larger clusters. The transition between these two regimes could be assigned to the transition of a planar to a spatial structure.

Although we have used the effective core potential for core electrons and explicit treatment for the valence electrons only, the obtained results show that it was accurate enough to pick up the essential physics. The present results can be useful for further theoretical and experimental investigation on the electronic properties of small aluminum clusters.

ACKNOWLEDGMENTS

This research was supported by CNPq, FAPESP, CAPES, and FUNAPE (Brazil).

*ladir@if.ufg.br
†jrabelo@if.ufg.br
‡dasilva_juarez@yahoo.com
§hai@ifsc.usp.br

[1] J. F. Jia, J. Z. Wang, X. Liu, Q. Xue, Z. Q. Li, Y. Kawazoe, and S. B. Zhang, Appl. Phys. Lett. **2002**, 3186 (2002).
[2] W. A. Heer, Rev. Mod. Phys. **65**, 611 (1993).
[3] M. Brack, Rev. Mod. Phys. **65**, 677 (1993).
[4] H. Haberland, *Cluster of Atoms and Molecules I* (Springer, Berlin, 1994).
[5] H. Haberland, *Cluster of Atoms and Molecules II* (Springer, Berlin, 1994).
[6] D. E. Bergeron, A. W. Castleman Jr., T. Morisato, and S. N. Khanna, Science **304**, 84 (2004).

[7]Y.-K. Han and J. Jung, J. Am. Chem. Soc. **130**, 2 (2008).
[8]P. J. Roach, W. H. Woodward, and A. W. Castleman Jr., Science **323**, 492 (2009).
[9]B. Cao, A. K. Starace, O. H. Judd, and M. F. Jarrold, J. Am. Chem. Soc. **131**, 2446 (2009).
[10]A. K. Starace, B. Cao, O. H. Judd, I. Bhattacharyya, and M. F. Jarrold, J. Chem. Phys. **132**, 034302 (2010).
[11]A. C. Reber, S. N. Khanna, P. J. Roach, W. H. Woodward, and A. W. Castleman Jr., J. Am. Chem. Soc. **129**, 16098 (2007).
[12]D. M. Cox, D. J. Trevor, R. L. Whetten, and A. kaldor, J. Phys. Chem. **92**, 421 (1988).
[13]K. J. Taylor, C. L. Pettiette, M. J. Craycraft, O. Chesnovsky, and R. E. Smalley, Chem. Phys. Lett. **152**, 347 (1988).
[14]C.-Y. Cha, G. Gantefor, and W. Eberhardt, J. Chem. Phys. **100**, 995 (1993).
[15]X. Li, H. Wu, X-B. Wang, and L.-S. Wang, Phys. Rev. Lett. **81**, 1909 (1998).
[16]J. Sun, W. C. Lu, H. Wang, Z.-S. Li, and C.-C. Sun, J. Phys. Chem. A **110**, 2729 (2006).
[17]R. O. Jones, Phys. Rev. Lett. **67**, 224 (1991).
[18]Y. L. Zhao and R. J. Zhang, J. Phys. Chem. A **111**, 7189 (2007).
[19]R. O. Jones, J. Chem. Phys. **99**, 1194 (1993).
[20]B. K. Rao and P. Jena, J. Chem. Phys. **111**, 1890 (1999).
[21]Z. Wu, M. D. Allendorf, and J. C. Grossman, J. Am. Chem. Soc. **131**, 13918 (2009).
[22]P. Hohenberg and W. Kohn, Phys. Rev. **136**, B864 (1964).
[23]W. Kohn and L. J. Sham, Phys. Rev. **140**, A1133 (1965).
[24]J. P. Perdew, J. A. Chevary, S. H. Vosko, K. A. Jackson, M. R. Pederson, D. J. Singh, and C. Fiolhais, Phys. Rev. B **46**, 6671 (1992).
[25]J. P. Perdew, K. Burke, and M. Ernzerhof, Phys. Rev. Lett. **77**, 3865 (1996).
[26]P. E. Blöchl, Phys. Rev. **50**, 17953 (1994).
[27]G. Kresse and J. Hafner, Phys. Rev. B **48**, 13115 (1993).
[28]G. Kresse and J. Furthmüller, Phys. Rev. B **54**, 11169 (1996).
[29]A. Walsh and J. L. F. Da Silva, and S.-H. Wei, Chem. Mater. **21**, 5119 (2009).
[30]M. J. Piotrowski, P. Piquini, and J. L. F. Da Silva, Phys. Rev. B **81**, 155446 (2010); J. L. F. DaSilva, H. G. Kim, M. J. Piotrowski, M. J. Prieto, and G. Tremiliosi-Filho, *ibid*. **82**, 205424 (2010).
[31]M. J. Frish *et al*., GAUSSIAN03, *Revision C.02*, Gaussian, Inc., Wallingford CT (2004).
[32]D. Feller, J. Comput. Chem. **17**, 1571 (1996); K. L. Schuchardt, B. T. Didier, T. Elsethagen, L. Sun, V. Gurumoorthi, J. Chase, J. Li, and T. L. J. Windus, Chem. Inf. Model. **47**, 1045 (2007).
[33]R. J. Needs, M. D. Tgowler, N. D. Drummond, and P. Lopes Rios, J. Phys.: Condensed Matter **22**, 023201 (2010).
[34]J. R. Trail and R. J. Needs, J. Chem. Phys. **122**, 174109 (2005); **122**, 014112 (2005).
[35]D. M. Ceperley and B. J. Alder, Phys. Rev. Lett. **45**, 566 (1980); W. M. C. Foulkes, L. Mitas, R. J. Needs, and G. Rajagopal, Rev. Mod. Phys. **73**, 33 (2001).
[36]G. Kresse and D. Joubert, Phys. Rev. B **59**, 1758 (1999).
[37]R. Hoppe, Angew. Chem. Internat. Edit. **9**, 25 (1970).
[38]R. Hoppe, Z. Kristallogr. **150**, 23 (1979).
[39]J. L. F. Da Silva, A. Walsh, and S.-H. Wei, Phys. Rev. B **80**, 214118 (2009).
[40]J. L. F. Da Silva, H. G. Kim, M. J. Piotrowski, M. J. Prieto, and G. Tremiliosi-Filho, Phys. Rev. B **82**, 205424 (2010).